Geological Society of America
Special Paper 416
2006

Calcrete features and age estimates from U/Th dating: Implications for the analysis of Quaternary erosion rates in the northern limb of the Sierra Nevada range (Betic Cordillera, southeast Spain)

J.M. Azañón
Departamento de Geodinámica, Universidad de Granada, 18071 Granada, Spain, and *Instituto Andaluz de Ciencias de la Tierra, CSIC-Universidad de Granada, 18071 Granada, Spain*

P. Tuccimei
Dipartimento di Scienze Geologiche, Universitá Roma Tre, 00146 Roma, Italy

A. Azor
Departamento de Geodinámica, Universidad de Granada, 18071 Granada, Spain

I.M. Sánchez-Almazo
Centro Andaluz de Medio Ambiente (CEAMA), Universidad de Granada, 18071 Granada, Spain

A.M. Alonso-Zarza
Departamento de Petrología y Geoquímica, Facultad de Ciencias Geológicas, Universidad Complutense, 28040 Madrid, Spain

M. Soligo
Dipartimento di Scienze Geologiche, Universitá Roma Tre, 00146 Roma, Italy

J.V. Pérez-Peña
Departamento de Geodinámica, Universidad de Granada, 18071 Granada, Spain

ABSTRACT

The Guadix topographic depression is a Neogene-Quaternary basin located in the central sector of the Betic Cordillera at the boundary between the South Iberian margin and the Alboran domain. This topographic depression is a plateau with an average elevation of 1000 m in the northern limb of the Sierra Nevada range. The continental deposits infilling the Guadix basin span time from the late Tortonian to the Pleistocene, when a laminar calcrete developed on fine- to coarse-grained fluvial and lacustrine deposits. The drainage pattern is strongly incised (up to 200 m) below the calcrete layer. Four coeval subsamples from the top laminae of the calcrete were collected and dated by the U/Th method. The resulting date is 42.6 ± 5.6 ka, which indicates the minimum age for the cessation of active sedimentation in the Guadix basin. Using this age, we have calculated the incision and erosion rates for the late Pleistocene to present-day time span in the Arroyo de Gor, a highly incised canyon in the eastern border of the Guadix basin. The minimum incision rates in this canyon are around 4 mm/yr. We envisage the capture of the Pliocene-Pleistocene endorheic

Azañón, J.M., Tuccimei, P., Azor, A., Sánchez-Almazo, I.M., Alonso-Zarza, A.M., Soligo, M., and Pérez-Peña, J.V., 2006, Calcrete features and age estimates from U/Th dating: Implications for the analysis of Quaternary erosion rates in the northern limb of the Sierra Nevada range (Betic Cordillera, southeast Spain), *in* Alonso-Zarza, A.M., and Tanner, L.H., eds., Paleoenvironmental Record and Applications of Calcretes and Palustrine Carbonates: Geological Society of America Special Paper 416, p. 223–239, doi: 10.1130/2006.2416(14).

Guadix basin by the Guadalquivir River after 42 ka as the main factor triggering the formation of the present-day eroded landscape. After the capture, the combination of climatic (wet periods), lithological (soft and loose sediments), and topographic (high average altitude) features allowed the development of the present-day entrenched drainage pattern.

Keywords: calcretes, U/Th dating, stable isotopes, Quaternary incision rates, river capture, Guadix basin, Betic Cordillera, SE Spain.

RESUMEN

La depresión de Guadix es una cuenca neógeno-cuaternaria situada en el sector central de la Cordillera Bética cubriendo el contacto entre el Margen Sudibérico y el Dominio de Alborán. Esta depresión topográfica es, sin embargo, una superficie elevada (sobre unos 1000 m) desarrollada en el flanco N de Sierra Nevada. El relleno continental de la cuenca de Guadix abarca desde el Tortoniense superior al Pleistoceno, y está coronado por una calcreta laminar que se desarrolló sobre materiales detríticos lacustres y fluviales. La red de drenaje está fuertemente encajada (hasta 200 m) bajo este nivel de calcretas. Se han datado, mediante el método de U/Th, cuatro sub-muestras correspondientes a las facies laminares situadas en el techo del nivel de calcretas más alto. El resultado de la datación de la calcreta es 42.6 ± 5.6 ka, que puede interpretarse como la edad mínima para el final de la sedimentación activa en la cuenca de Guadix. Usando esta edad como referencia, hemos calculado las tasas de incisión y erosión desde el Pleistoceno superior en el Arroyo de Gor, un cañón fuertemente encajado en el borde oriental de la cuenca de Guadix. Las tasas de incisión en este cañón están alrededor de 4 mm/año. Consideramos que la captura Pliocena-Pleistocena (post–42 ka) de la cuenca, con carácter endorreico en ese momento, por parte del río Guadalquivir es el principal factor desencadenante del actual relieve erosivo que presenta la cuenca de Guadix. Tras la captura, la combinación de factores climáticos (periodos húmedos), litológicos (sedimentos detríticos con escasa cohesión) y topográficos (alta altitud media) han favorecido el encajamiento progresivo de la red de drenaje actual.

Palabras clave: calcretas, datación U/Th, Isótopos estables, tasas de incisión cuaternaria, captura fluvial, Cuenca de Guadix, Cordilleras Béticas, SE España.

INTRODUCTION

Quaternary calcretes are widespread in many ancient terrestrial basins from all over the world, including Australia (Arakel, 1986), southern Africa (Watts, 1980; Nash and McLaren, 2003), northwestern America (Machette, 1985), and southern Europe, especially Spain (Alonso-Zarza et al., 1998a). In the case of the Spanish Quaternary calcretes, they occur either in aggradational regimes interbedded with alluvial sediments (Jiménez-Espinosa and Jiménez-Millán, 2003), or, most commonly, in degradational regimes on different terrace levels (Sancho et al., 2004). In both cases, detailed studies of the calcretes have provided most valuable data that illuminate rates of fluvial aggradation, fluvial incision, climatic regime, and even tectonic activity. Additionally, Quaternary calcretes cap the sedimentary infill of some of the mostly terrestrial Cenozoic basins in Spain, such as the Ebro basin (Sancho and Meléndez, 1992) and the Teruel basin (Alonso-Zarza and Arenas, 2004). In these cases, thick laminar calcretes constitute the last material accumulated at the top of the sedimentary sequences, which are incised by the present-day fluvial network. Further to the south and southeast, thick calcrete profiles also formed at the top of some Neogene-Quaternary basins in the Betic Cordillera (Dumas, 1969; Kelly et al., 2000; Candy et al., 2003; García et al., 2003; Nash and Smith, 2003). Calcrete formation in the Betic Neogene-Quaternary basins predates the incision of the present-day fluvial network, thus, if dated radiometrically, its presents a potentially useful geomorphic tool to establish incision rates of the main rivers.

Precise dating of pedogenic carbonates either by ^{14}C or U/Th series has proved to be a useful tool to establish both the chronology of sequences of terraces and incision rates in SE Spain (Kelly et al., 2000; Candy et al., 2004). Moreover, the radiometric date

of pedogenic carbonates, together with oxygen and carbon stable isotope studies, is of paramount importance in establishing Quaternary paleoclimatic regimes.

In this paper, we use a multidisciplinary approach to study a calcrete layer developed at the top of the sedimentary infilling of the Guadix basin in SE Spain (Figs. 1 and 2). The calcrete constitutes a flat geomorphic surface in which the present-day drainage network is entrenched. U/Th dating and stable isotope analyses of the top laminae in this calcrete have provided us with a radiometric age and allowed us to propose a paleoclimatic setting for the development of this surface. Moreover, a detailed petrographic study of the calcrete reveals different vadose-phreatic phases previous to or coeval with the initial stages of river incision. Finally, we draw on the radiometric age obtained to estimate the incision rates of the present-day drainage network, while also addressing the possible causes behind the relatively high values calculated. A brief description of each technique or method used in this study will be provided in the appropriate context.

GEOLOGICAL SETTING

The area of study is located in the Betic Cordillera in southeastern Spain (Fig. 1), which represents a tectonically active region related to the collision between Africa and Iberia (DeMets et al., 1994; Morales et al., 1999; Galindo-Zaldívar et al., 1999, 2003). Despite this general compressional tectonic setting, the main tectonic and geomorphic features of the Betic Cordillera are related to extensional tectonics (e.g., Galindo-Zaldívar et al., 1989; García-Dueñas et al., 1992; Crespo-Blanc et al., 1994; Martínez-Martínez and Azañón, 1997; Martínez-Martínez et al., 2002). In this context, the present-day topography of the Betic Cordillera can be described as a succession of mountain ranges and basins dissected by the main rivers, which incised both the ranges and the basins (Fig. 2A). The highest range in the Betic Cordillera is the Sierra Nevada, which has been recently interpreted as an elongated dome resulting from the interference of two orthogonal fold systems: one due to a rolling-hinge mechanism in the footwall of a WSW-directed extensional detachment and the other due to coeval N-S compression (Martínez-Martínez et al., 2004). The Sierra Nevada (and other neighboring ranges) emerged in middle Miocene times, progressively isolating different intramontane basins, such as the Granada and the Guadix-Baza basins (Fig. 2A). Long-term uplift rates in this region are low to moderate (0.02–0.3 mm/yr) according to present-day altitudes of shallow-marine Miocene and Pliocene sediments (Braga et al., 2003; Silva et al., 2003; Booth-Rea et al., 2004; Sanz de Galdeano and Alfaro, 2004).

The Guadix-Baza basin is one of the intramontane Neogene-Quaternary basins of the Betic Cordillera (Figs. 1 and 2), located in the central part of the orogen between the external (South Iberian margin) and the internal (Alboran domain) zones. The present-day topography of this basin corresponds to a depression bounded by ranges (Fig. 2). The continental infilling of this basin spans from the latest Tortonian to the Pleistocene (Vera, 1970; Peña, 1979; Viseras, 1991; Fernández et al., 1996). From a paleogeographical point of view, the Guadix-Baza basin can be viewed in Pliocene-Pleistocene times as an endorheic depression surrounded by mountains. The sedimentary record of Pliocene-Pleistocene age suggests the existence at the marginal parts of the Guadix basin of alluvial systems, which flowed into a central lake (Viseras, 1991; Viseras and Fernández, 1992). In the eastern and southern borders of the Guadix subbasin (Guadix basin henceforth), the continental infill is represented by alternating poorly cemented conglomerates and sands of Pliocene-Pleistocene age

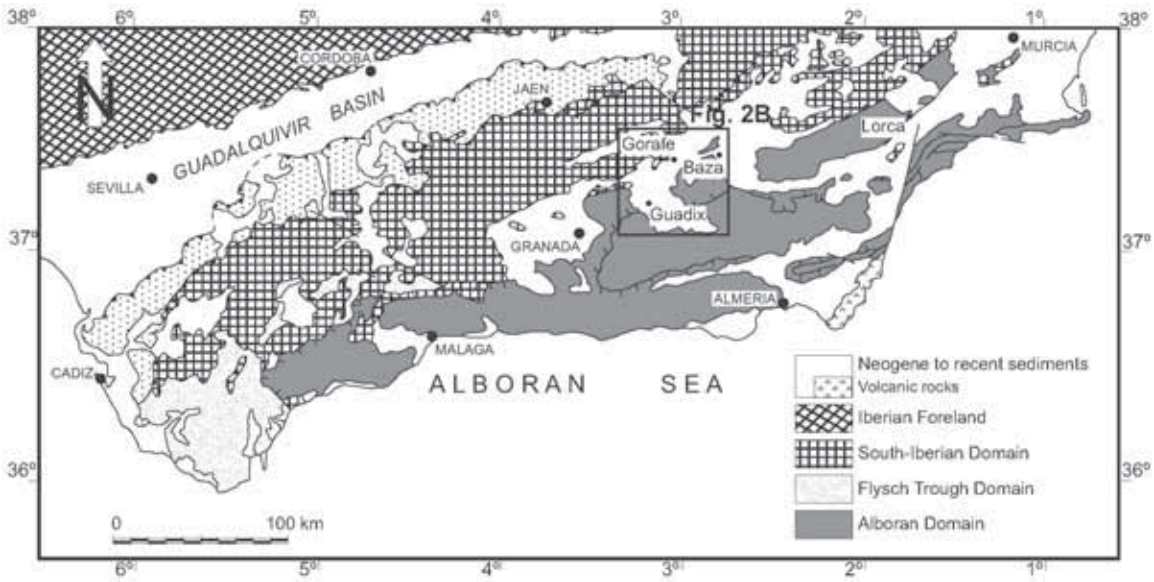

Figure 1. Geological setting of the Guadix-Baza basin in the Betic Cordillera (SE Spain).

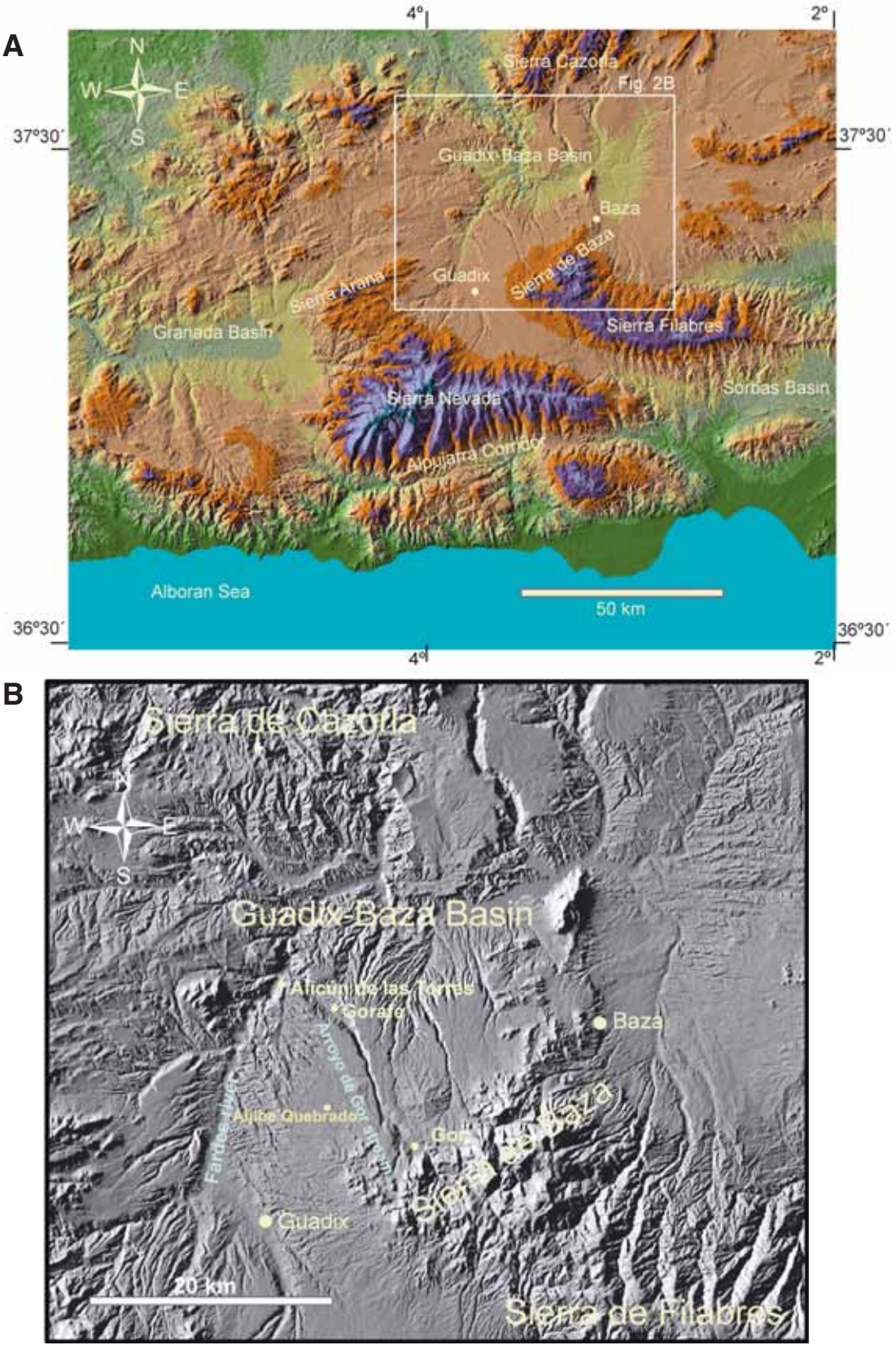

Figure 2. (A) Topographic sketch of the eastern Betic Cordillera with the locations of the main basin and mountain ranges. (B) Digital elevation model (DEM) of the Guadix basin (see location in Figures 1 and 2A), where the main geomorphic features (elevated flat surface defined by the calcrete, badland areas, and main streams) can be observed.

(Viseras, 1991). The conglomeratic layers are dominant toward the upper part of the sequence and are capped by a 0.5–1-m-thick calcrete, which outcrops in a widespread area of the Guadix basin (Fig. 3). Toward the center of the basin, the conglomerates and sands grade laterally to lacustrine deposits represented by marls and clays. These marly sediments are also capped by the calcrete layer. The uppermost outcropping layers of the lacustrine deposits in the Baza subbasin have been dated by amino acid racemization on ostracodes, yielding ages around 280 ka (Ortiz et al., 2004). The lacustrine layers dated in the Baza subbasin

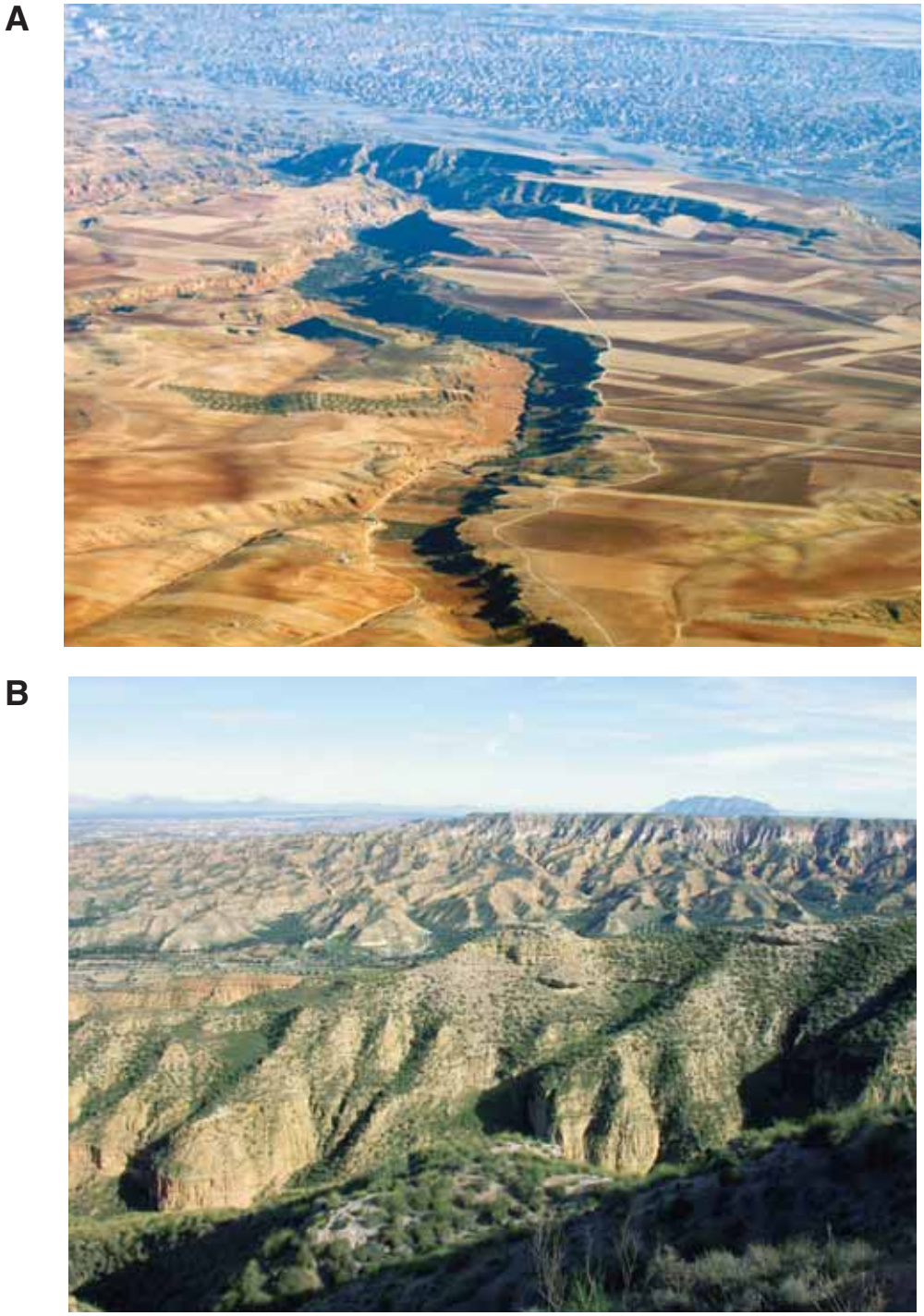

Figure 3. (A) Oblique aerial view looking north of the surface defined by the calcrete into which canyon-shaped streams incise. Note the badlands in the upper part of the image (photograph by Javier Sanz de Galdeano). (B) Photograph of the Pliocene-Pleistocene stratigraphic sequence of the Guadix basin capped by the calcrete layer defining the flat surface.

occupy a stratigraphic position lower than the top calcrete layer. The calcrete and the associated geomorphic surface are less well preserved in the Baza subbasin, outcropping only at the margins, near the surrounding mountain ranges.

GEOMORPHOLOGY OF THE GUADIX BASIN

While forming a topographic depression, the Guadix basin has at present an external drainage to the Atlantic Ocean through the Guadalquivir River. The main mountain ranges surrounding the Guadix basin are the Sierra Nevada to the south, Sierra de Baza to the east, Sierra Cazorla to the north, and Sierra Arana to the west (Fig. 2A). The basin itself is an elevated (average altitude around 1000 m) plateau capped by the calcrete layer (Fig. 3). The flat geomorphic surface defined by the calcrete is strongly dissected by canyons and a main trunk river with a well-developed floodplain, the Fardes River (Fig. 2B). At present, most of the streams in this area have an ephemeral hydraulic regime with no discharge most of the time punctuated by episodic flooding events caused by heavy rains. This hydrology is controlled by the present-day climate in this region, which is semiarid, with an average annual rainfall between 300 and 350 mm. The only river with permanent discharge is the Fardes River.

The flat surface defined by the calcrete is mostly horizontal (Fig. 3), except at the margins of the basin, where it inclines slightly basinward. This surface of regional extent represents the end of the sedimentation in the Guadix basin and was developed under a soil covering the underlying fluvial and lacustrine deposits (see next section). The calcrete layer formed prior to the present-day external drainage pattern, when the Guadix basin was still an endorheic catchment area. Thus, the calcrete marks a residual surface of an old flat area that lacked well-organized streams and extended throughout the entire Guadix basin.

After the formation of the above-mentioned surface, the former Pleistocene endorheic Guadix basin must have been captured by the Guadalquivir River (Calvache and Viseras, 1997), thus starting the development of the present-day strongly entrenched drainage pattern. The capture was probably caused by headward erosion of the Guadalquivir River, favored by the topographically elevated position of the Guadix basin. Thus, the capture can be viewed, via a base-level lowering, as the triggering factor responsible for the formation of the present-day eroded landscape. Furthermore, the erosion would not have been a coeval process throughout the basin. Instead, once the Guadix basin was captured by the Guadalquivir River, an incision wave would have progressed headward along the basin, eventually reaching its southern margin. At the margins of the Guadix basin, the flat elevated surface marked by the calcrete appears dissected by a few narrow and rectilinear canyons (Fig. 3A), such as the Arroyo de Gor (Fig. 2B). Toward the north and northwest, the landscape is much more eroded and dominated by gullies and pipes (Vandekerckhove et al., 2000, 2003), with some buttes being the only remains of the flat geomorphic surface.

A second and lower flat surface corresponds to the present-day cultivated floodplain of the Fardes River, the main river draining the Guadix basin (Fig. 2B). This main axial valley does not run in a central position along the Guadix basin, but rather close to its western border. The Fardes River is the only one in the Guadix basin with terrace deposits at its margins. In one locality (Alicún de las Torres; Fig. 2B), three terrace levels made up of travertine deposits can be recognized at one margin of the Fardes River.

In summary, three main geomorphic domains can be distinguished in the Guadix basin (Figs. 2 and 3): (1) the flat elevated surface cut by canyons; (2) the intermediate steep badland area; and (3) the lower surface of the Fardes floodplain.

THE CALCRETE

Profile and Micromorphology

The calcrete constitutes the top of the Pliocene-Pleistocene sedimentary sequence, featuring a very continuous, but heterogeneous, layer along the Guadix basin. Up to three different calcrete layers can be observed, depending on the locality. The maximal thickness of each layer is around 1.5 m, and nonweathered clastic deposits are intercalated between the calcrete layers, as in the Aljibe Quebrado section (Fig. 4). This section is the most complete—it is composed of three layers of laminar calcrete up to 20 cm thick (Fig. 4). The calcrete layers are developed on top of

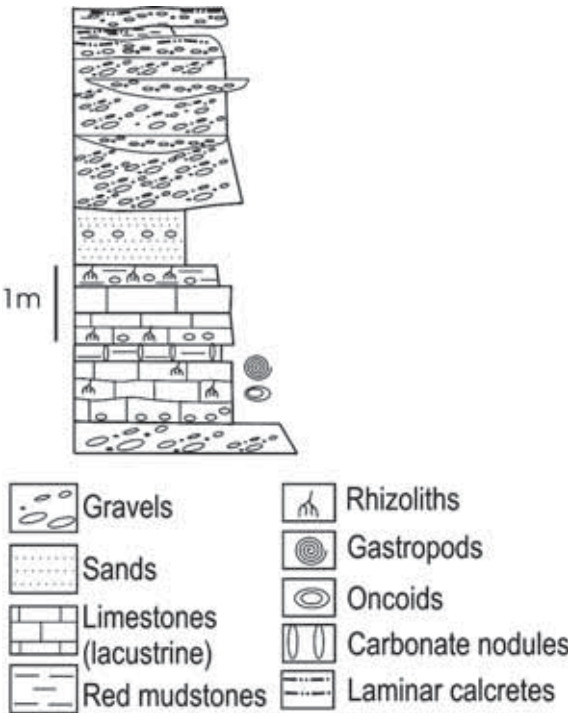

Figure 4. Aljibe Quebrado section showing the transition from palustrine deposits to the studied calcretes (at the top).

a thick gravel bed with intercalated red mudstones at the upper part. In other sections, such as in the Arroyo de Gor, the calcrete consists of a single layer around 1 m thick (Fig. 5), developed on brown silts with gravel clasts. In this locality, the single calcrete layer, in turn, includes three main horizons, which from bottom to top are: nodular, massive, and laminar.

At the macroscale, this three-horizon pattern is observed throughout the Guadix basin. The nodular horizon is ~30 cm thick and occurs at the base of the calcrete profiles. The host rocks are red mudstones in which spheroidal to cylindrical carbonate nodules are present. The nodules consist of homogeneous micrite with some floating sand grains, representing calcification

Figure 5. View of the top calcrete at Arroyo de Gor. Several indurated laminar horizons can be seen.

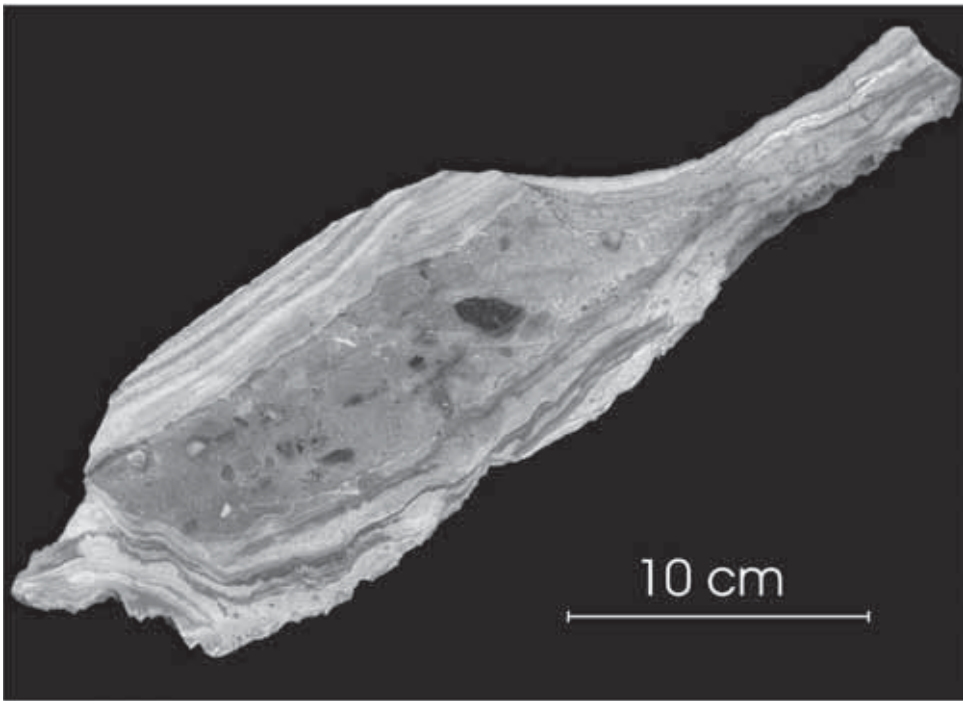

Figure 6. Hand sample of the uppermost part of the calcrete layer at the Arroyo de Gor. The laminae coat all the gravel bed. The indurated gravel constitutes, in this case, the massive horizon.

around roots. The massive horizon is decimeter-scale and consists of polygenic rock fragments (Fig. 6) incorporated in a dense and hard red micrite matrix. This matrix shows nonbiogenic features, such as desiccation cracks and floating etched detrital grains. Nevertheless, biogenic features are dominant and include root traces, calcified root cells, calcite spheres, vadose pisoliths, and micritic peloids. Moreover, coarse calcite mosaics, either as cement or as a result of recrystallization and displacement, are common. The laminar horizon occurs at the uppermost part of the profiles, in some cases constituting a sort of fine-grained detrital jacket around the uppermost part of the nodular horizon (Figs. 6 and 7). This horizon consists of alternating of light and dark laminae. The dark laminae contain more detrital grains and show alveolar septal structures as well as lines of calcite crystals, probably indicating calcified root structures (Alonso-Zarza et al., 1998b). The light laminae are richer in micrite and have fewer detrital grains, although they have more clay (sepiolite or palygorskite) minerals. These light laminae also contain spherulites, calcified root spheres, and needle fiber calcite (Figs. 7 and 8). In those cases in which the laminar horizon envelops the massive one, there are also vadose-gravitational cements underlying the lowermost laminae. This fact probably indicates the progressive lowering of local-scale hanging water tables.

The macro- and microfeatures described above are indicative of a pedogenic calcrete, where roots must have played an important role, as evidenced by the occurrence of calcified root traces and alveolar septal structures. The presence of spherulites may be taken to indicate that cyanobacterial mats (Verrecchia et al., 1995) developed at the top part of the profiles. The alternation of laminae with different proportions of detrital grains and biogenic features suggests successive small-scale periods of sedimentation, erosion, and soil formation in the uppermost part

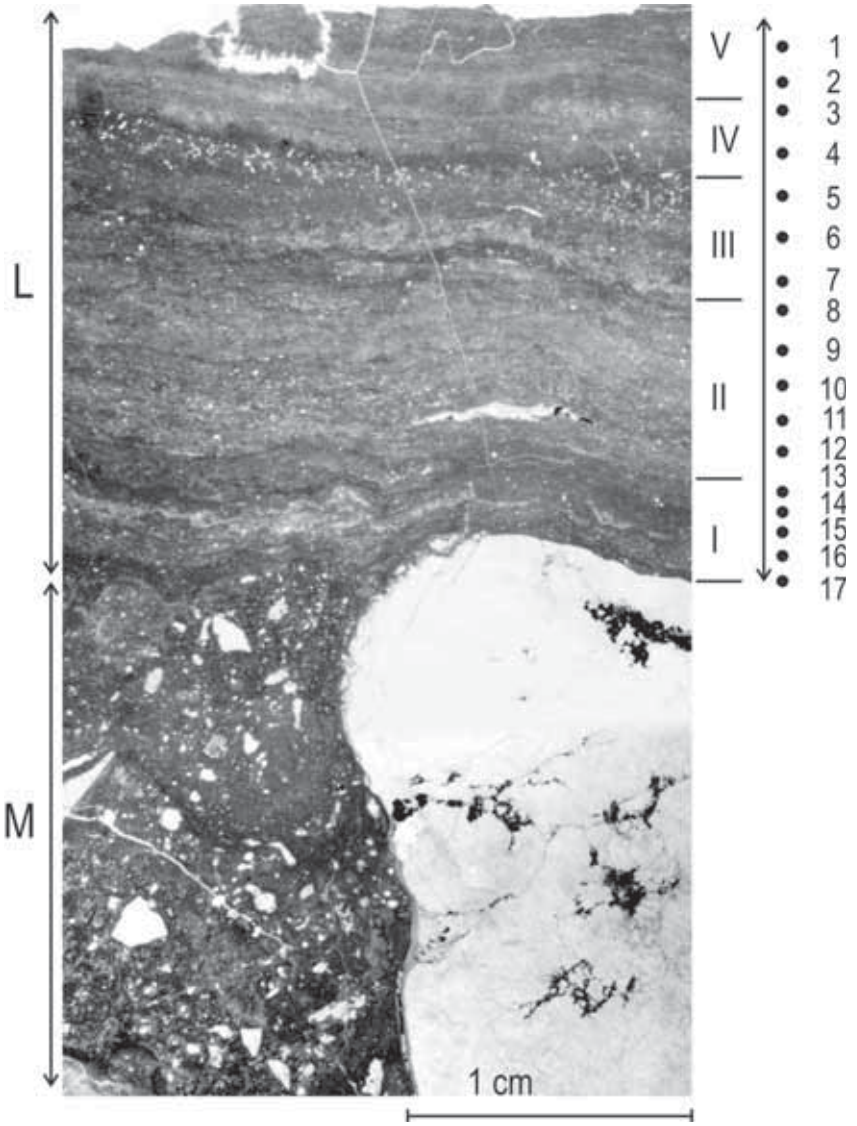

Figure 7. View of the sample drilled for stable isotope characterization of the laminar horizon with locations of the different points of analysis. Massive (M) and laminar (L) horizons are easily separated. Massive horizons are very rich in etched detrital clasts. The different zones (I–V) within the laminar horizon are also indicated. See text for further explanations.

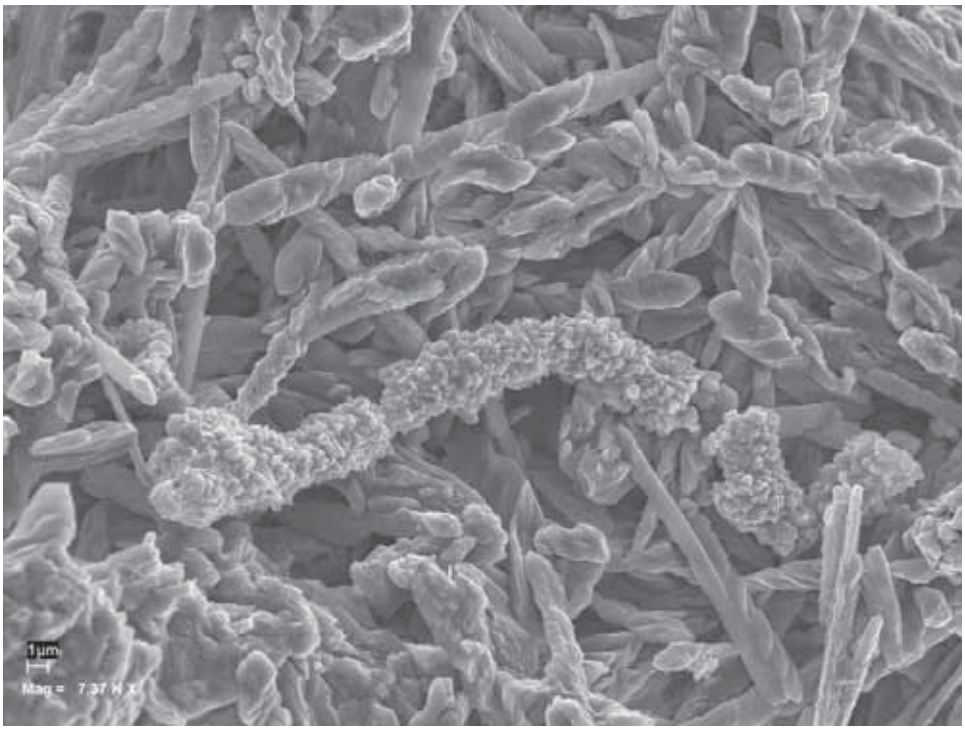

Figure 8. Scanning electron microscope (SEM) view in which needle fiber calcite crystals and calcified filaments form most of the laminae with alveolar septal structure.

of a relatively stable surface. These sedimentation–erosion–soil-forming periods might be related to climate-vegetation changes (Alonso-Zarza and Silva, 2002). The overall features of the calcrete indicate that it was formed due to the influence of a sparse vegetation cover of bushes and shrubs developed under a semi-arid climate. This is the context deduced for the formation of similar calcretes in Spain (Alonso-Zarza et al., 1998a) and all over the world (Mack and James, 1994; Alonso-Zarza, 2003).

Stable Isotope Geochemistry

We performed a stable isotope study of 17 samples drilled from the uppermost centimeters of the laminar calcrete horizon (Figs. 7 and 9). The powder samples were baked under vacuum at 360 ºC for 30 min to remove any organic matter. The stable isotope analyses were performed at Cambridge University (UK), using a Micromass Multicarb Sample Preparation System attached to a VG Isotech PRIMS mass spectrometer. The isotope data are reported according to Vienna Peedee belemnite (VPDB) international standards. The precision of the results is better than ±0.06‰ for $^{12}C/^{13}C$ and ±0.08‰ for $^{16}O/^{18}O$.

The values of $\delta^{18}O$ and $\delta^{13}C$ (Figs. 9 and 10) vary from –9.17‰ to –6.28‰ and from –11.18‰ to –6.36‰ (VPDB), respectively. These values fall within the ranges described for calcretes by Alonso-Zarza (2003) in a recent and detailed review of the paleoenvironmental significance of palustrine and pedogenic carbonates. As a whole, our results reveal a considerable variation of $\delta^{13}C$, greater than that of $\delta^{18}O$, which seems to be a common feature in calcretes (Alonso-Zarza, 2003; Alonso-Zarza and Arenas, 2004). Both $\delta^{18}O$ and $\delta^{13}C$ show several fluctuations from the bottom to the top of the profile, although the general trend is toward heavier values upward (Fig. 9). Moreover, there is a strong positive correlation between $\delta^{13}C$ and $\delta^{18}O$ ($r^2 = 0.89$; Fig. 10).

The stable isotope composition of pedogenic carbonates has proved to be a powerful tool for paleoenvironmental studies (Cerling, 1984; Cerling and Quade, 1993; Alam et al., 1997) and has been used to reconstruct climate and vegetation changes through time (Ding and Yang, 2000; Fox and Koch, 2003, 2004; Alonso-Zarza and Arenas, 2004; Sanyal et al., 2004). Values of $\delta^{18}O$ in calcretes depend on both the stable isotopic composition of soil water (Cerling, 1984; Cerling and Quade, 1993) and temperature. The $\delta^{18}O$ of soil water, in turn, is related to the isotopic composition of local rainfall, which also is strongly controlled by temperature (Cerling and Quade, 1993). Additionally, evaporation in the uppermost horizons of the soil can also affect $\delta^{18}O$ values in pedogenic carbonates and result in $\delta^{18}O$ enrichment (Cerling and Quade, 1993). In the samples studied, the general $\delta^{18}O$ trend toward heavier values higher in the profile (Fig. 9) might be taken to indicate a tendency toward aridity at the final stages of calcrete development.

The values of $\delta^{18}O$ obtained enable us to estimate the isotopic composition of the rain water during the initial stages of formation of the laminar calcrete. To do so, we have applied the equation proposed by Jiamao et al. (1997), which relates $\delta^{18}O$ of pedogenic carbonate to $\delta^{18}O$ of rainfall and also includes the effect of evaporation (Zanchetta et al., 2000). The resulting $\delta^{18}O$ value for rain water at the time when the laminar calcrete started to develop is –10.12‰, i.e., a value 2.63‰ lower than that of

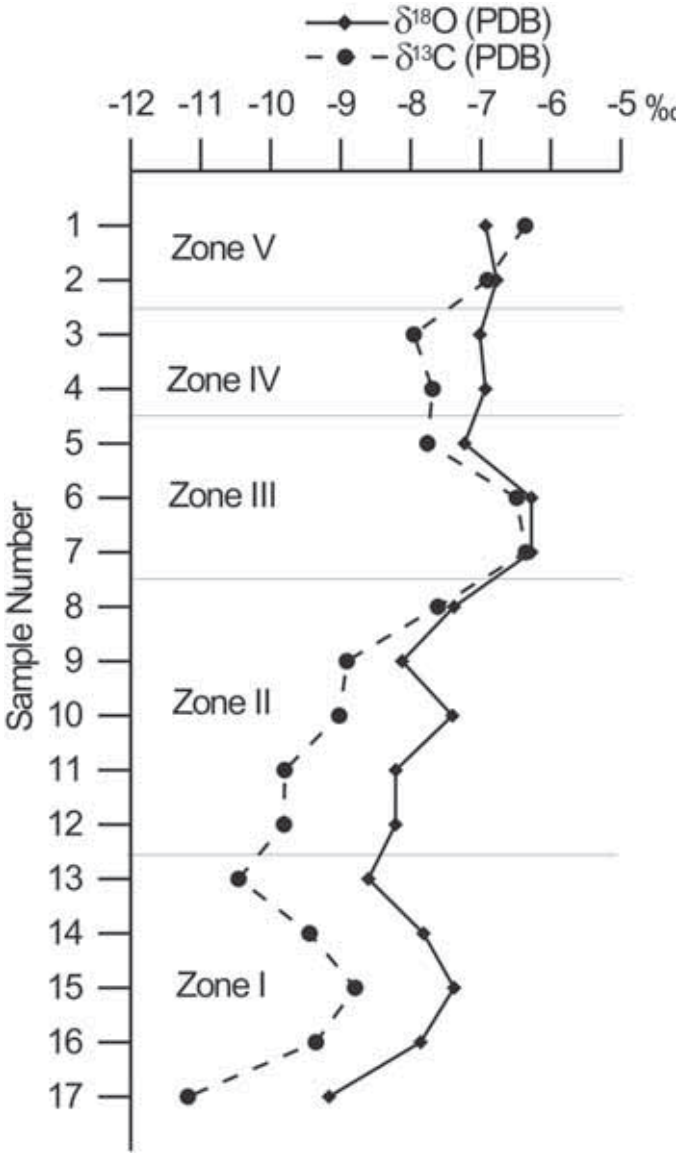

Figure 9. $\delta^{18}O$ and $\delta^{13}C$ in the top laminar calcrete. The isotope values are referenced to the Pee Dee belemnite (PDB) standard. See location of the samples in Figure 7. The different zones (I–V) within the laminar horizon are also indicated.

present-day rain water (–7.49‰; Caballero et al., 1996). These lighter $\delta^{18}O$ values in rain water could indicate that the climate was cooler than present during the formation of the calcrete.

The $\delta^{13}C$ of pedogenic carbonate depends on the isotopic composition of soil CO_2 (Quade et al., 1989), which, in turn, is related to the composition of the local vegetation (Cerling, 1984). Thus, $\delta^{13}C$ of pedogenic carbonate is controlled mainly by the ratio of C_4/CAM (Crassulacean acid metabolism) to C_3 plants. C_3 plants (trees, most shrubs, and cool-season grasses) have lighter $\delta^{13}C$ values (about –27‰) than C_4 plants (about –12‰; Cerling and Quade, 1993). Consequently, when vegetation cover is dominated by C_3 plants, $\delta^{13}C$ in soil CO_2 is lower

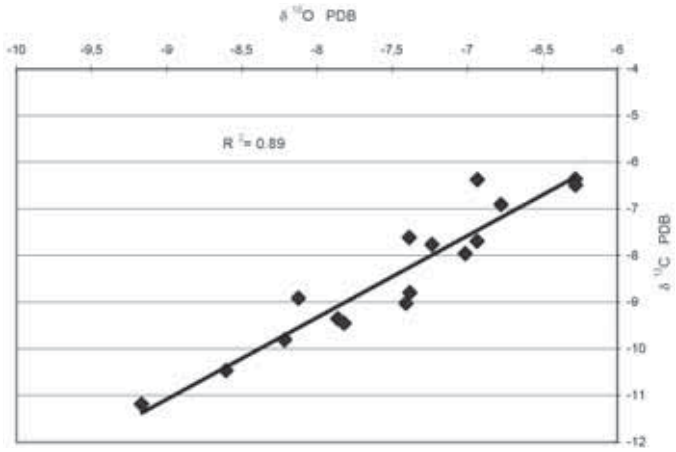

Figure 10. Relationship between $\delta^{18}O$ and $\delta^{13}C$ for the laminar calcrete.

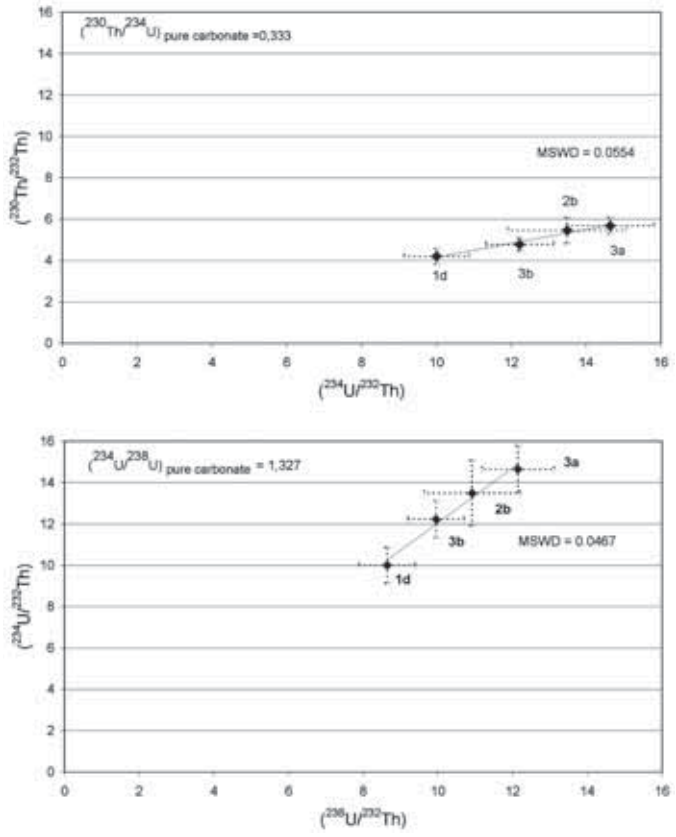

Figure 11. Calcrete isochron plots (2-dimensional versions) based on total dissolution of four coeval subsamples, with 1σ error crosses. The slopes in the ($^{234}U/^{232}Th$)-($^{238}U/^{232}Th$) and ($^{230}Th/^{232}Th$)-($^{234}U/^{232}Th$) diagrams represent the ($^{234}U/^{238}U$) and ($^{230}Th/^{234}U$) activity ratios, respectively, of the pure carbonate. MSWD—mean square of weighted deviates. 1d, 3b, 2b, and 3a are subsamples that have been used in the isochron calculation.

than when C_4 plants dominate (Cerling, 1984; Alonso-Zarza, 2003). The respective distributions and abundances of C_3 and C_4 plants are controlled by climate. C_4 plants are adapted to high water stress and elevated temperatures; their relative abundance has been used as an index of past aridity (Jiamao et al., 1997). In contrast, C_3 plants prefer cool temperatures during the growing season and live at present at high latitudes (Alam et al., 1997; Ding and Yang, 2000). On these grounds, several authors have established that the $\delta^{13}C$ values of pedogenic carbonate which formed at 25 ºC from pure C_4 and C_3 biomasses are approximately +2‰ and –12‰, respectively (Cerling, 1984; Alam et al., 1997). After comparing these values with $\delta^{13}C$ in the calcrete studied here (–11.18‰ to –6.36‰), we conclude that C_3 plants dominated the local ecosystem during the calcrete formation period. Similarly, the trend to higher $\delta^{13}C$ values higher in the profile can be interpreted as a response to changing vegetation, with an increase in C_4 plants due to a substantial increase in aridity. In the same way, the positive correlation between $\delta^{18}O$ and $\delta^{13}C$ (Fig. 10) can be related to increasing aridity during the final stages of calcrete formation. This is commonly true during the formation of pedogenic carbonates (Cerling, 1984).

A comparison between the petrographic features and the stable isotope record in the laminar calcrete enables us to characterize five different zones, which are from bottom to top as follows (Figs. 7 and 9): (I) mostly laminar calcrete with alveolar structures, which have average $\delta^{18}O$ and $\delta^{13}C$ of –8.18‰ and –9.85‰, respectively; (II) a laminated zone characterized by the presence of laminae very rich in quartz silt, with average $\delta^{18}O$ of –7.87‰ and $\delta^{13}C$ of –9.03‰, where the quartz laminae correspond to the heaviest values in $\delta^{18}O$ and $\delta^{13}C$ within this zone; (III) massive micrite, with the heaviest isotope values in all of the profile; and (IV) and (V) two laminated zones, with average $\delta^{18}O$ of –6.97‰ for 4 and –6.85‰ for 5. The $\delta^{13}C$ values are –7.82‰ for 4 and –6.64‰ for 5.

Zones I and II have the lighter values, indicating the development of a vegetation cover, probably under the least arid conditions in the entire profile. Quartz-rich laminae (with the heaviest isotopic composition) may indicate an increase of aridity and maybe an eolian dust influx. Zone III corresponds to the most arid conditions and probably the least biogenic control on the carbonate precipitated in the soil zone. The last two zones (IV and V) have similar $\delta^{18}O$ values, thus pointing to a more stable climate, although the vegetation cover could be slightly different than in the lower part of the calcrete.

In short, both micromorphology and stable isotope features are related to the climatic conditions prevailing during the formation of the different calcrete laminae. Generally, the massive micritic laminae with the heaviest isotope values represent the most arid conditions, which, in turn, indicate inhibited biogenic activity. Conversely, the occurrence of alveolar septal structures in zones with the lightest isotope values (I and II) is related to a wider vegetation cover under less arid climate.

U/Th Dating

Four coeval subsamples of the very top laminar horizon of the calcrete were collected and dated by the U/Th isochron method (Bischoff and Fitzpatrick, 1991). The analytical basis for dating calcretes is the measurement of the ^{230}Th formed by the decay of authigenic ^{234}U and, indirectly, ^{238}U, the uranium having been co-precipitated from solution with the carbonate (Kelly et al., 2000). Calcretes are, however, impure mixtures of calcium carbonate and incorporated detrital minerals, resulting in the same radionuclides being present in both the authigenic and detrital fractions. Our approach is to use an isochron method to determine the authigenic radionuclide component and, on the basis of this, its age (Bischoff and Fitzpatrick, 1991). The subsamples are assumed to be mixtures, in different proportions, of homogeneous detrital and authigenic carbonate end members. This method has been successfully applied to calcrete dating from alluvial terraces in the Sorbas basin (Kelly et al., 2000; Candy et al., 2004).

The samples were cut with a diamond saw in order to remove the altered parts, then crushed and washed ultrasonically in deionized water. The fragments were checked with a stereoscopic microscope to identify and discard any recrystallized portions. About 20 g of each subsample were dissolved in an HCl-HNO_3-HF mixture, following the standard "total dissolution" method outlined by Bischoff and Fitzpatrick (1991) and Luo and Ku (1991). After dissolution, isotopic complexes of uranium and thorium were extracted according to the procedure described by Edwards et al. (1987) and alpha-counted using high-resolution ion implanted Ortec silicon surface barrier detectors at the Radiochemistry Laboratory of Roma Tre University (Italy). A standardized ^{232}U-^{228}Th tracer was used as a yield monitor, and a correction was made for the presence of detrital ^{228}Th and in-growth of ^{224}Ra. $^{228}Th/^{232}Th$ equilibrium was checked on an unspiked subsample. The ($^{230}Th/^{234}U$) and ($^{234}U/^{238}U$) activity ratios of the authigenic fraction were calculated from the slope of a 3-dimensional isochron fitted to the *x*-*y*-*z* data ($^{238}U/^{232}Th$, $^{230}Th/^{232}Th$, $^{234}U/^{232}Th$) using the method of minimum likelihood estimation, outlined by Ludwig and Titterington (1994), in which the analytical data are weighed for analytical errors and error correlations. The corresponding age was determined from these authigenic fraction activity ratios using ISOPLOT, a plotting and regression program for radiogenic isotope data (Ludwig, 2003). The analytical data are given in Table 1, and the isochron diagrams are shown in Figure 11. The calculated age uncertainties are expressed as 1σ. The probability that the uncertainty in the age is due to the analytical errors alone is quantified through the calculation of the mean square of weighted deviates (MSWD). A high probability (or MSWD < 1; Fig. 11) indicates that, in this case, the uncertainty regarding the age is due only to analytical errors rather than to other sources of geological origin, e.g., subsamples are not coeval or mixture end members are not homogeneous. The resulting date is 42.6 ± 5.6 ka (Table 1), which indicates the age of the very top laminar part of the calcrete and thus gives a minimum time for the cessation of active sedimentation in the Guadix basin.

TABLE 1. ANALYTICAL DATA FOR CALCRETE SUBSAMPLES, GUADIX, SPAIN

Subsample	(^{234}U/^{232}Th)	(^{238}U/^{232}Th)	(^{230}Th/^{232}Th)	(^{234}U/^{238}U)carb	(^{230}Th/^{234}U)carb.	Age (ka)
1d	10.005 ± 0.867	8.641 ± 0.753	4.205 ± 0.383			
2b	13.492 ± 1.577	10.912 ± 1.281	5.455 ± 0.630	1.358 ± 0.132	0.328 ± 0.036	42.6 ± 5.6
3a	14.647 ± 1.161	12.144 ± 0.971	5.684 ± 0.407			
3b	12.229 ± 0.909	9.950 ± 0.748	4.776 ± 0.309			

Note: Errors are quoted as 1σ. (^{230}Th/^{234}U)carb and (^{234}U/^{238}U)carb are referenced to the pure carbonate authigenic fraction used in the calculation of the age.

INCISION RATES

Estimating incision rates in fluvial environments is not an easy task due to the difficulties in establishing absolute ages of reference surfaces. Typically, local-scale, but not regional-scale, incision rates can be derived, since the processes causing entrenchment can be very variable throughout catchments through time and space. In this respect, it must be emphasized that river incision always progresses headward as a consequence of increasing stream power, which, in turn, can be due to base-level lowering and/or profile steeping. Therefore, a single river can incise at different times along its different reaches, thus propagating an incision wave headward. Moreover, rock resistance can be quite variable along a river and can also affect local-scale incision rates.

Taking into account the above drawbacks and using the age obtained for the calcrete as a reference, we have calculated incision and erosion rates for the late Pleistocene to present-day time span in the Guadix basin. These estimated rates can be considered as minimum values since the surface defined by the calcrete predates river entrenchment (see next section) and the process was not coeval throughout the basin, but probably progressed as an incision wave.

We made calculations for the Arroyo de Gor, a stream with well-known geomorphologic features. This stream is a 30-km-long canyon highly incised (up to 200 m) into the Pliocene-Pleistocene infill (including the capping calcrete layer) of the eastern border of the Guadix basin (Figs. 2B and 12). This canyon is characterized by the absence of terrace deposits and by an abundance of large-scale rotational slides (Azañón et al., 2005). The present-day morphology of the Arroyo de Gor is the result of a combination of entrenchment, fracturing, and landsliding. The initial deep entrenchment of the stream is attributed to the base-level lowering related to the capture of the former endorheic Guadix basin by the Guadalquivir river in the late Pleistocene, i.e., after the formation of the calcrete layer at 42 ka. This river incision created a canyon with unstable subvertical walls, which, due to gravitational instability, give way to vertical open tension cracks at some distance from the canyon edge. The rotational slides are thought to have occurred during heavy rains by a combination of piping, which lengthened the tension cracks, and infiltration, thus reducing the shear strength along the subhorizontal lithological contact between conglomerates and underlying clays (Azañón et al., 2005).

The rock volume remobilized by erosion in the Arroyo de Gor has been calculated from a digital elevation model (DEM) with a resolution of 1 pixel per 20 m (Fig. 12). The canyon volume was estimated with the aid of ArcGis 8.2 by counting the number of pixels between a top level defined by the flat geomorphic surface formed by the calcrete and the topography. The resulting volume of rock remobilized by erosion in the Arroyo de Gor is 7972 m^3 ha^{-1}. With these data, the estimation of the erosion rate is 15.62 m^3 ha^{-1} yr^{-1} or 28 t ha^{-1} yr^{-1} (assuming an average density of 1.8 t/m^3 for the sedimentary infilling). Thus, the average minimum vertical incision rates in this canyon are around 4 mm/yr. Realistically, these average rates probably underestimate the actual values, since the Arroyo de Gor had almost reached its present morphology before 6 ka, as indicated by the presence of dolmens of that age built on the landslide bodies (Azañón et al., 2005). After the dolmens were built at around 6 ka, the canyon was 30–50 m into the landslide bodies, which yields a minimum Holocene vertical incision rate of roughly 5–7 mm/yr. This more recent rate is naturally higher than the average minimum rate calculated for the last 42 ka (around 4 mm/yr). Moreover, the Arroyo de Gor was developed by an initial vertical entrenchment of ~150 m that must have occurred prior to the large-scale landsliding, which, in turn, enlarged the initially very narrow canyon (Azañón et al., 2005). The age of the initial vertical entrenchment is unknown, having occurring sometime between the capture of the former endorheic Guadix basin by the Guadalquivir River and the large-scale landsliding, i.e., between 42 and 6 ka. With these observations in mind, we tentatively hypothesize that the river capture and the subsequent vertical entrenchment and landsliding could have occurred in a period between 38 and 28 ka, when several millennial-scale episodes (Is8 to Is3) of higher mean annual rainfall (up to 900 mm) occurred (Sánchez Goñi et al., 2002). Assuming that both the vertical entrenchment of 150 m and the large-scale landsliding were completed during this 10 k.y. period, the real rates of vertical incision for that period may have been as high as 15 mm/yr, i.e., 3–4 times higher than the average minimum rates.

DISCUSSION

The continental infill in the Guadix basin ended with the formation of a calcrete layer, which extends some hundreds of square kilometers and defines a flat elevated surface. Four coeval carbonate subsamples from the top laminae of the calcrete have been dated by the U/Th method, yielding an age of 42.6 ± 5.6 ka. This datum is in accordance with other ages obtained on the uppermost alluvial-lacustrine layers of the Guadix-Baza basin,

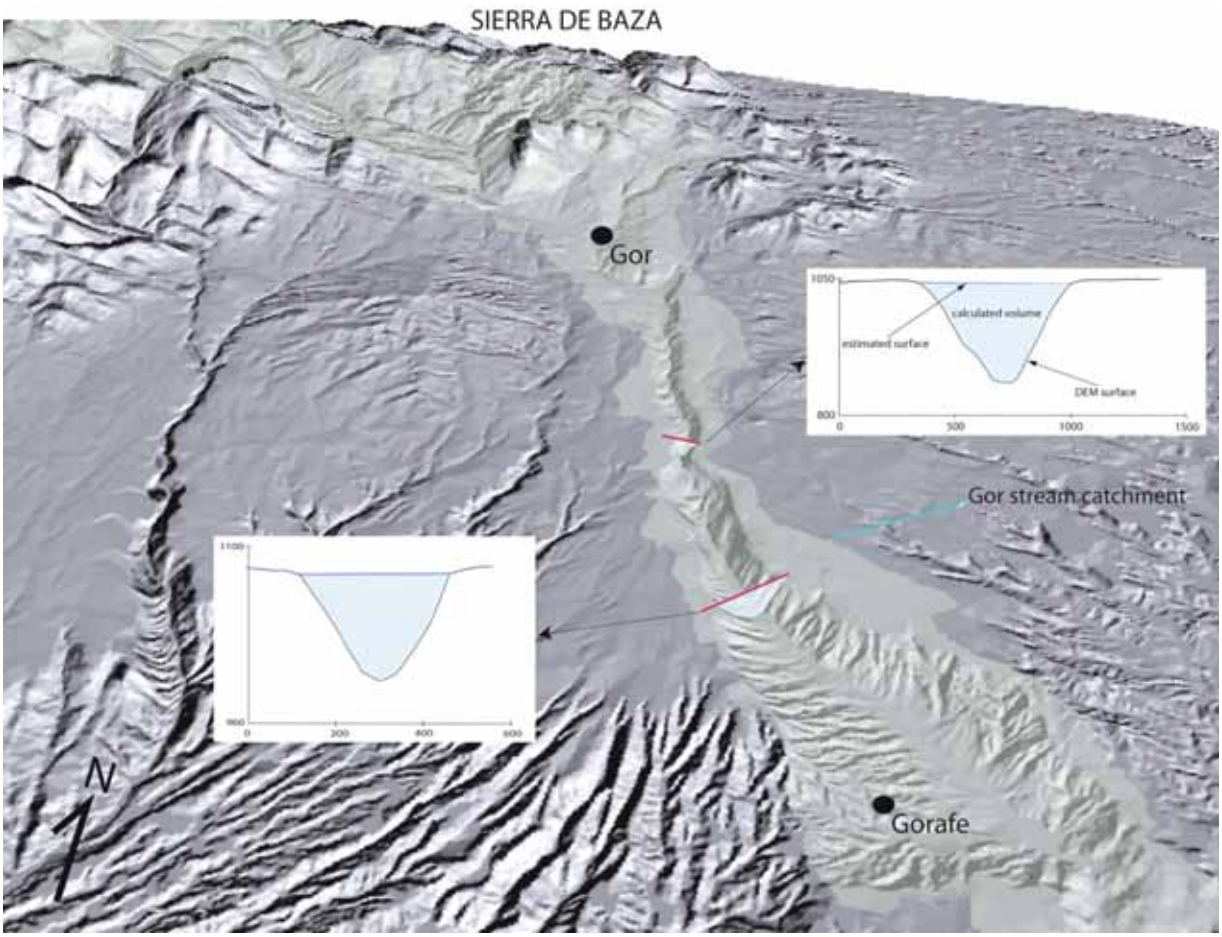

Figure 12. Digital elevation model (DEM) of the Arroyo de Gor stream. Calculations of volume eroded have been performed on this DEM with the aid of ArcGis 8.2, using the geomorphic surface defined by the calcrete and the topography of the canyon as reference.

namely, an amino acid racemization age of 280 ka (Ortiz et al., 2004) and an age of 100 ka estimated for archaeological activity coeval to the most recent deposits (Botella et al., 1985, 1986, cited in Calvache and Viseras, 1997). These dates correspond to stratigraphic levels located below the calcrete layer investigated here. Therefore, the age of 42.6 ka is a more accurate estimation for the end of the sedimentation in the Guadix basin, since the calcrete layer is at the very top of the stratigraphic sequence. The regional extent of the calcrete and the lack of any observable relationship between lateral facies variation within the calcrete and the present-day stream distribution prove that the present-day drainage pattern formed later than calcrete formation, i.e., later than final sedimentation in the Guadix basin. Moreover, the Pliocene-Pleistocene sedimentary facies distribution shows that there is no spatial coincidence between present-day streams and Pliocene-Pleistocene paleorivers.

The petrographic features and the stable isotope geochemistry of the calcrete indicate a pedogenic origin under a semiarid climate in which vegetation was sparse and dominated by bushes and shrubs. Variations in humidity and vegetation cover are indicated by changes in both micromorphology and isotopic composition in the top laminar calcrete. In general, the better-laminated zones that include more alveolar features are the isotopically lighter, both in carbon and oxygen, whereas the more massive zones are the heaviest. The results of the stable isotope study enable us to propose that during the initial stages of laminar calcrete formation, the climate was cooler than it is today, and aridity increased upward, when the sedimentation was ending.

Some inferences can be made by considering the age obtained for the calcrete (42.6 ± 5.6 ka) in conjunction with the paleoclimatic conditions deduced from its petrographic and stable isotope geochemical features. In this regard, calcrete formation approximately coincides with the H5 and H4 Heinrich events (Dansgaard et al., 1993), which correspond to millennial-scale variations in atmospheric temperatures over Greenland. These events have been identified in the recent stratigraphic record of the Alboran Sea and have been related to sharp changes in surface water temperature (Pérez-Folgado et al., 2003), as well as to rapid vegetation shifts in Southern Iberia (Sánchez Goñi et al., 2002). According to these authors, H5 and H4 were characterized by a very arid climate with an average annual rainfall of ~300 mm and average winter temperatures 10 ºC cooler than present

day. We hypothesize that calcrete formation in the Guadix basin occurred during these extremely dry and cold climatic periods.

Calcretes have been used as a basis for establishing relative landform chronologies in Quaternary alluvial sequences of the eastern Betic Cordillera (Harvey et al., 1995, 1999; Kelly et al., 2000). These chronologies, in turn, have been used to determine the rates of operation of geomorphic processes over the Quaternary period. However, a detailed calcrete micromorphological analysis must be carried out before using calcrete layers as chronomorphologic gauges (Candy et al., 2003). Particularly, Candy et al. (2003) highlighted that the pedogenic- or groundwater-linked character of the calcretes is of paramount importance for the geomorphic analysis. In this respect, the age derived for a typical pedogenic calcrete, such as the top layer of the Guadix basin, marks the end of the continental infill, when the basin was still endorheic and the present-day drainage pattern had not yet developed. In contrast, a groundwater calcrete would be much more ambiguous in terms of sedimentologic and geomorphic significance, because its formation would be related either to the final sedimentation or to the subsequent development of the present-day drainage pattern. Therefore, the calcrete layer studied here constrains both the age of the capture of the former endorheic Guadix basin by the Guadalquivir River and the minimal values of incision rates in this area.

Using the age of the calcrete as a reference, we have calculated minimum incision and erosion rates for the late Pleistocene to present-day time span in the Guadix basin. In fact, estimations were performed for a canyon-shaped stream (the Arroyo de Gor) with well-known geomorphic features. The significance of the resulting incision rates, particularly whether they represent local (one single stream) or regional (the whole basin) values, must be discussed according to the geomorphic features of the Guadix basin. In this regard, we first highlight the homogeneous river incision throughout the Guadix basin, i.e., both the Fardes River and the Arroyo de Gor canyon have been incised to approximately the same depth in the flat surface defined by the calcrete. Nevertheless, the Fardes River attests to a more complicated evolution, including the formation of several terrace levels and a very intense lateral erosion with development of a badland landscape. Furthermore, the 30-km-long Arroyo de Gor itself, which represents half the length of the Guadix basin, is incised into a bedrock with homogeneous resistance and lacks important gradient variations. Thus, despite the fact that river incision would progress as a headward wave along the Arroyo the Gor, the values obtained, always considered minimums and subject to several uncertainties, can be viewed reasonably as regional-scale incision rates.

Average minimum incision rates in the Arroyo de Gor stream are around 4 mm/yr. These values are relatively high (up to ten times higher) compared to available Pleistocene-Holocene incision rates, also minimum values, obtained in other Neogene-Quaternary basins of the Betic Cordillera: 0.1–0.4 mm/yr in the Sorbas basin (Mather and Harvey, 1995; Kelly et al., 2000), 0.3–0.7 mm/yr in the Alpujarra Corridor (García et al., 2004), and 0.1–0.7 mm/yr in the Granada basin (Martín-Martín et al., 2001). A number of factors, such as lithologies, stream piracy, climate, topography, and tectonics, can be invoked as being responsible for the high incision rates in the Guadix basin. A closer comparison with the other basins reduces these factors to three, namely, stream piracy, topography, and tectonics, since the lithologies and the climate are quite homogeneous in all the Neogene-Quaternary basins of the Betic Cordillera. Stream piracy, via the capture of a former endorheic basin by a river with a lower base level, namely sea level, can be assumed to have occurred during the Quaternary in all of the aforementioned basins. The timing of the capture, as well as the site where it took place, would notably influence the local-scale incision rates and the upstream progression of the incision wave. Nevertheless, drawing on the quite similar erosive state of these basins, one can reasonably consider that the late Quaternary incision waves have progressed headward comparably in all of them, reaching the surrounding mountain areas. Thus, at first glance, the high incision rates in the Guadix basin are probably related to the high average altitude (around 1000 m). This, in addition to the poorly indurated lithologies, would facilitate fast incision of the rivers during episodic heavy rains. In contrast, the Sorbas basin and the Alpujarra Corridor (Fig. 2A) have an average altitude of less than 400 m, which accounts for the low estimated incision rates. In the case of the Granada basin (Fig. 2A), which has an average altitude around 600 m, one would expect intermediate incision rates. The reason for the low values (quite similar to the ones of the Sorbas basin and the Alpujarra Corridor) cannot be justified solely on the basis of the difference in altitude between the Guadix and the Granada basins (see following discussion).

Several issues must be discussed in regard to the possible contribution of tectonic activity to the high incision rates. First of all, the incision rates estimated for the Guadix basin are one or two orders of magnitude higher than the long-term regional uplift rates (0.02–0.3 mm/yr), calculated from the ages of marine deposits (Braga et al., 2003; Silva et al., 2003; Booth-Rea et al., 2004; Sanz de Galdeano and Alfaro, 2004). In the case of the Guadix basin, an uplift rate of 0.15 mm/yr, corresponding to the late Tortonian to present-day period, can be estimated according to the altitude of shallow-marine deposits of that age preserved at its southern border. The absence of marine deposits younger than the late Tortonian precludes the estimation of uplift rates for shorter time spans. Nevertheless, drawing on geological and seismological evidence, the possibility of very high uplift rates for the late Pleistocene to Holocene period can be reasonably discarded. In this respect, two salient aspects must be emphasized: (1) no faults with Pleistocene-Holocene activity are observed to affect the infill of the Guadix basin or its borders, and (2) both present-day and historical seismicity is concentrated to the south (Granada basin, Alpujarra Corridor) and east (Lorca basin, Fig. 1) of the Guadix basin (Morales et al., 1999; Mancilla et al., 2002; Muñoz et al., 2002; Serrano et al., 2002). Therefore, it can be concluded that the high late Pleistocene to Holocene incision rates in the Guadix basin do not represent a response to an accelerated

tectonic activity during the Quaternary. Nevertheless, the high average altitude of the Guadix basin is probably related to large-scale long-term isostatic uplift after the pre-Miocene crustal thickening in the Betic Cordillera. Interestingly, the only sector of the Betic Cordillera with a present-day crustal thickness exceeding 35 km is the Guadix basin and the Sierra Nevada (Banda et al., 1993). Therefore, we suggest that sustained isostatic uplift may be responsible for maintaining the high average altitude of the Guadix basin, while also facilitating the estimated high incision rates.

We have argued before that the differences in elevation do not seem great enough to account for the considerably different Pleistocene-Holocene incision rates. At a greater scale, some differences in the tectonic activity could be the main reason for the different incision rates between the Guadix and the Granada basin. The Granada basin is bounded to the east by the western Sierra Nevada mountain front, which is thought to be one of the main active areas in all of the Betic Cordillera. This mountain front is marked by NW-SE–oriented, SW-dipping normal faults with Quaternary activity and present-day seismicity (Sanz de Galdeano et al., 2003; Azañón et al., 2004). The Granada basin is located in the hanging wall of this active normal-fault system; thus, it is undergoing Quaternary tectonic subsidence, which would preclude high rates of river incision. In contrast, the Guadix basin, together with the whole Sierra Nevada, constitutes a single block located in the footwall of this active normal-fault system, and thus it is subjected to tectonic and/or isostatic uplift.

CONCLUSIONS

The Guadix basin is a very special landscape when compared with other Neogene-Quaternary basins in the Betic Cordillera. It represents an elevated plateau strongly incised by the drainage pattern. Moreover, this landscape seems to be the result of a very fast incision process of the main rivers dissecting the geomorphic surface marked by the 42 ka calcrete layer. We envisage the capture of the Pliocene-Pleistocene endorheic Guadix basin by the Guadalquivir River during the late Pleistocene as the starting point for the formation of this landscape. This capture was probably a climatically driven process that must have occurred under wetter (and also possibly warmer) conditions than the present-day semiarid climate. Sánchez Goñi et al. (2002) described several millennial-scale episodes (Is8 to Is3) between 38 and 28 ka with a mean annual rainfall up to 900 mm during which the basin capture could have occurred. Undoubtedly, the capture process was facilitated by the high average altitude of the Guadix basin. Thus, the capture can be considered as an isostatically assisted process, since the high elevation of the Guadix basin seems to be in part the result of long-term large-scale isostatic uplift. After the capture, the combination of climatic, lithological, and topographic features would have facilitated the development of the present-day entrenched drainage pattern.

ACKNOWLEDGMENTS

The research reported in this work has been financed by the Spanish Ministry of Education with Fondos Europeos de Desarrollo Regional funds of the European Union, through grants numbers REN2001-3378, CGL2004-03333/BTE, and CGL2004-04342/BTE. Comments and suggestions by Pablo Silva and an anonymous reviewer are kindly acknowledged. We thank Francisco Gonzálvez García for reviewing our English text.

REFERENCES CITED

Alam, M.S., Keppens, E., and Paepe, R., 1997, The use of oxygen and carbon isotope composition of pedogenic carbonates from Pleistocene palaeosols in NW Bangladesh, as palaeoclimatic indicators: Quaternary Science Reviews, v. 16, p. 161–168, doi: 10.1016/S0277-3791(96)00044-3.

Alonso-Zarza, A.M., 2003, Palaeoenvironmental significance of palustrine carbonates and calcretes in the geological record: Earth-Science Reviews, v. 60, p. 261–298, doi: 10.1016/S0012-8252(02)00106-X.

Alonso-Zarza, A.M., and Arenas, C., 2004, Cenozoic calcretes from the Teruel Graben, Spain: Microstructure, stable isotope geochemistry and environmental significance: Sedimentary Geology, v. 167, p. 91–108, doi: 10.1016/j.sedgeo.2004.02.001.

Alonso-Zarza, A.M., and Silva, P.G., 2002, Quaternary laminar calcretes with bee nests: Evidences of small scale climatic fluctuations, eastern Canary Islands, Spain: Palaeogeography, Palaeoclimatology, Palaeoecology, v. 178, p. 119–135, doi: 10.1016/S0031-0182(01)00405-9.

Alonso-Zarza, A.M., Silva, P., Goy, J.L., and Zazo, C., 1998a, Fan-surface dynamics and biogenic calcrete development: Interactions during ultimate phases of fan evolution in the semiarid SE Spain (Murcia): Geomorphology, v. 24, p. 147–167, doi: 10.1016/S0169-555X(98)00022-1.

Alonso-Zarza, A.M., Sanz, M.E., Calvo, J.P., and Estévez, P., 1998b, Calcified root cells in Miocene pedogenic carbonates of the Madrid Basin: Evidence for the origin of *Microcodium* b: Sedimentary Geology, v. 116, p. 81–97, doi: 10.1016/S0037-0738(97)00077-8.

Arakel, A.V., 1986, Evolution of calcrete in palaeodrainages of the Lake Narpperby area, Central Australia: Palaeogeography, Palaeoclimatology, Palaeoecology, v. 54, p. 283–303, doi: 10.1016/0031-0182(86)90129-X.

Azañón, J.M., Azor, A., Booth-Rea, G., and Torcal, F., 2004, Small-scale faulting, topographic steps and seismic ruptures in the Alhambra (Granada, SE Spain): Journal of Quaternary Science, v. 19, p. 219–227, doi: 10.1002/jqs.838.

Azañón, J.M., Azor, A., Pérez-Peña, J.V., and Carrillo, J.M., 2005, Late Quaternary large-scale rotational slides induced by river incision: The Arroyo de Gor area (Guadix basin, SE Spain): Geomorphology v. 69, p. 152–168.

Banda, E., Gallart, J., García-Dueñas, V., Dañobeitia, J.J., and Makris, J., 1993, Lateral variation of the crust in the Iberian Peninsula: New evidence from the Betic Cordillera: Tectonophysics, v. 221, p. 53–66, doi: 10.1016/0040-1951(93)90027-H.

Bischoff, J.L., and Fitzpatrick, J.A., 1991, U-series dating of impure carbonates: An isochron technique using total sample dissolution: Geochimica et Cosmochimica Acta, v. 55, p. 543–554, doi: 10.1016/0016-7037(91)90011-S.

Booth-Rea, G., Azañón, J.M., Azor, A., and García-Dueñas, V., 2004, Influence of strike-slip fault segmentation on drainage evolution and topography: A case study: The Palomares fault zone (southeastern Betics, Spain): Journal of Structural Geology, v. 26, p. 1615–1632, doi: 10.1016/j.jsg.2004.01.007.

Botella, M., Martínez, C., and Cárdenas, F.J., 1985, Las industrias paleolíticas de Cueva Horá (Darro, Granada): Antropología y Paleoecología Humana, v. 1, p. 59–74.

Botella, M., Martínez, C., Cárdenas, F.J., and Cañabate, M.J., 1986, Industria musteriense y achelense de Cueva Horá (Darro, Granada): Book in Honour of Luis Siret: Granada, Spain, Junta de Andalucía, p. 79–95.

Braga, J.C., Martín, J.M., and Quesada, C., 2003, Patterns and average rates of late Neogene–Recent uplift of the Betic Cordillera: SE Spain: Geomorphology, v. 50, p. 3–26, doi: 10.1016/S0169-555X(02)00205-2.

Caballero, E., Jiménez de Cisnero, C., and Reyes, E., 1996, A stable isotope

study of cave seepage waters: Applied Geochemistry, v. 11, p. 583–587, doi: 10.1016/0883-2927(96)00026-1.

Calvache, M.L., and Viseras, C., 1997, Long-term control mechanisms of stream piracy processes in southeast Spain: Earth Surface Processes and Landforms, v. 22, p. 93–105, doi: 10.1002/(SICI)1096-9837(199702)22:2<93::AID-ESP673>3.0.CO;2-W.

Candy, I., Black, S., Sellwood, B.W., and Rowan, J.S., 2003, Calcrete profile development in Quaternary alluvial sequences, southeast Spain: Implications for using calcretes as a basis for landform chronologies: Earth Surface Processes and Landforms, v. 28, p. 169–185, doi: 10.1002/esp.445.

Candy, I., Black, S., and Sellwood, B.W., 2004, Quantifying time scales of pedogenic calcrete formation using U-series disequilibria: Sedimentary Geology, v. 170, p. 177–187, doi: 10.1016/j.sedgeo.2004.07.003.

Cerling, T.E., 1984, The stable isotopic composition of modern soil carbonate and its relationship to climate: Earth and Planetary Science Letters, v. 71, p. 229–240, doi: 10.1016/0012-821X(84)90089-X.

Cerling, T.E., and Quade, J., 1993, Stable carbon and oxygen isotopes in soil carbonates, *in* Swart, P.K., Lohmann, K.C., Mckenzie, J.A., and Savin, F., eds., Climate Change in Continental Isotopic Records: Washington, D.C., American Geophysical Union Geophysical Monograph 78, p. 217–231.

Crespo-Blanc, A., Orozco, M., and García-Dueñas, V., 1994, Extension versus compression during the Miocene tectonic evolution of the Betic chain: Late folding of normal fault systems: Tectonics, v. 13, p. 79–88, doi: 10.1029/93TC02231.

Dansgaard, W., Johnsen, S.J., Clausen, H.B., Dahl-Jensen, D., Gunderstrup, N.S., Hammer, C.V., Hvidberg, C.S., Steffensen, J.P., Sveinbjornsdottin, A.E., Jouzel, J., and Bard, G., 1993, Evidence for general instability of past climate from 250 kyr ice-core record: Nature, v. 364, p. 218–220, doi: 10.1038/364218a0.

DeMets, C., Gordon, R.G., Argus, D.F., and Stein, S., 1994, Effect of recent revisions to the geomagnetic reversal time scale on estimates of current plate motions: Geophysical Research Letters, v. 21, p. 2191–2194, doi: 10.1029/94GL02118.

Ding, Z.L., and Yang, S.L., 2000, C_3/C_4 vegetation evolution over the last 7.0 Myr in the Chinese Loess Plateau: Evidence from pedogenic carbonate $\delta^{13}C$: Palaeogeography, Palaeoclimatology, Palaeoecology, v. 160, p. 291–299, doi: 10.1016/S0031-0182(00)00076-6.

Dumas, B., 1969, Glacis et croutes calcaires dans le levant Espagnol: Bulletin de l'Association de Geographes Français, v. 375–376, p. 553–561.

Edwards, R.L., Chen, J.H., and Wasserburg, G.J., 1987, ^{238}U-^{234}U-^{230}Th-^{232}Th systematics and the precise measurement of time over the past 500,000 years: Earth and Planetary Science Letters, v. 81, p. 175–192, doi: 10.1016/0012-821X(87)90154-3.

Fernández, J., Viseras, C., and Soria, J.M., 1996, Stratigraphic architecture of the Neogene basins in the central sector of the Betic Cordillera (Spain): Tectonic control and base-level changes, *in* Friend, P.F., and Dabrio, C., eds., Tertiary Basins of Spain: The Stratigraphic Record of Crustal Kinematics: Cambridge, UK, Cambridge University Press, p. 353–365.

Fox, D.L., and Koch, P.L., 2003, Tertiary history of C_4 biomass in the Great Plains, USA: Geology, v. 31, p. 809–812, doi: 10.1130/G19580.1.

Fox, D.L., and Koch, P.L., 2004, Carbon and oxygen isotopic variability in Neogene paleosol carbonates: Constraints on the evolution of the C_4-grasslands of the Great Plains, USA: Palaeogeography, Palaeoclimatology, Palaeoecology, v. 207, p. 305–329, doi: 10.1016/S0031-0182(04)00045-8.

Galindo-Zaldívar, J., González-Lodeiro, F., and Jabaloy, A., 1989, Progressive extensional shear structures in a detachment contact in the western Sierra Nevada (Betic Cordilleras, Spain): Geodinamica Acta, v. 3, p. 73–85.

Galindo-Zaldívar, J., Jabaloy, A., Serrano, I., Morales, J., González-Lodeiro, F., and Torcal, F., 1999, Recent and present-day stresses in the Granada basin (Betic Cordilleras): Example of a late Miocene–present-day extensional basin in a convergent plate boundary: Tectonics, v. 18, p. 686–702, doi: 10.1029/1999TC900016.

Galindo-Zaldívar, J., Gil, A.J., Borque, M.J., González Lodeiro, F., Jabaloy, A., Marín Lechado, C., Ruano, P., and Sanz de Galdeano, C., 2003, Active faulting in the internal zones of the central Betic Cordilleras (SE, Spain): Journal of Geodynamics, v. 36, p. 239–250, doi: 10.1016/S0264-3707(03)00049-8.

García, A.F., Zhu, Z., Ku, T.L., Sanz de Galdeano, C., Chadwick, O.A., and Chacón Montero, J., 2003, Tectonically driven landscape development within the eastern Alpujarran Corridor, Betic Cordillera, SE Spain (Almería): Geomorphology, v. 50, p. 83–110, doi: 10.1016/S0169-555X(02)00209-X.

García, A.F., Zhu, Z., Ku, T.L., Chadwick, O.A., and Chacón Montero, J., 2004, An incision wave in the geologic record, Alpujarran Corridor, southern Spain (Almería): Geomorphology, v. 60, p. 37–72, doi: 10.1016/j.geomorph.2003.07.012.

García-Dueñas, V., Balanyá, J.C., and Martínez-Martínez, J.M., 1992, Miocene extensional detachments in the outcropping basement of the northern Alboran basin (Betics) and their tectonic implications: Geo-Marine Letters, v. 12, p. 88–95, doi: 10.1007/BF02084917.

Harvey, A.M., Miller, S.Y., and Wells, S.G., 1995, Quaternary soil and river terrace sequences in the Aguas/Feos River systems: Sorbas basin, southeast Spain, *in* Lewin, J., Macklin, M.G., and Woodward, J.C., eds., Mediterranean Quaternary River Environments: Rotterdam, Balkema, p. 263–281.

Harvey, A.M., Goy, J.L., Stokes, M., Zazo, C., Silva, P.G., and Mather, A.E., 1999, The impact of Quaternary sea-level and climatic change on coastal alluvial fans in the Cabo de Gata ranges, southeast Spain: Geomorphology, v. 28, p. 1–22, doi: 10.1016/S0169-555X(98)00100-7.

Jiamao, H., Keppens, E., Tungsheng, L., Paepe, R., and Wenying, J., 1997, Stable isotope composition of the carbonate concretion in loess and climate change: Quaternary International, v. 37, p. 37–43, doi: 10.1016/1040-6182(96)00005-5.

Jiménez-Espinosa, R., and Jiménez-Millán, J., 2003, Calcrete development in Mediterranean colluvial carbonates systems from SE Spain: Journal of Arid Environments, v. 53, p. 479–489, doi: 10.1006/jare.2002.1061.

Kelly, M., Black, S., and Rowan, J.S., 2000, A calcrete-based U/Th chronology for landform evolution in the Sorbas basin, southeast Spain: Quaternary Science Reviews, v. 19, p. 995–1010, doi: 10.1016/S0277-3791(99)00050-5.

Ludwig, K.R., 2003, Mathematical-statistical treatment of data and errors for $^{230}Th/U$ geochronology, *in* Bourdon, B., Henderson, G.M., Lundstrom, C.C., and Turner, S.P., eds., Uranium-Series Geochemistry: Reviews in Mineralogy and Geochemistry, v. 52, p. 631–656.

Ludwig, K.R., and Titterington, D.M., 1994, Calculation of $^{230}Th/U$ isochrons, ages, and errors: Geochimica et Cosmochimica Acta, v. 58, p. 5031–5042, doi: 10.1016/0016-7037(94)90229-1.

Luo, S., and Ku, T.L., 1991, U-series dating: A generalised method employing total sample dissolution: Geochimica et Cosmochimica Acta, v. 55, p. 555–564, doi: 10.1016/0016-7037(91)90012-T.

Machette, M.N., 1985, Calcic soils of southwestern United States, *in* Weide, D.L., ed., Soil and Quaternary Geology of the Southwestern United States: Geological Society of America Special Paper 203, p. 1–21.

Mack, G.H., and James, W.C., 1994, Paleoclimate and the global distribution of paleosols: The Journal of Geology, v. 102, p. 360–366.

Mancilla, F.L., Ammona, C.J., Herrmann, R.B., and Morales, J., 2002, Faulting parameters of the 1999 Mula earthquake, southeastern Spain: Tectonophysics, v. 354, p. 139–155, doi: 10.1016/S0040-1951(02)00340-2.

Martín-Martín, M., Andreo, B., Martín-Algarra, A., and Julià, R., 2001, Travertinos del borde noreste de la Depresión de Granada, *in* Sanz de Galdeano, C., Peláez-Montilla, J.A., and López-Garrido, A.C., eds., La Cuenca de Granda: Estructura, Tectónica Activa, Geomorfología y Dataciones Existentes: Granada, Editorial Universidad de Granada, p. 22–28.

Martínez-Martínez, J.M., and Azañón, J.M., 1997, Mode of extensional tectonics in the southeastern Betics (SE Spain). Implications for the tectonic evolution of the peri-Alborán orogenic system: Tectonics, v. 16, p. 205–225, doi: 10.1029/97TC00157.

Martínez-Martínez, J.M., Soto, J.I., and Balanyá, J.C., 2002, Orthogonal folding of extensional detachments: Structure and origin of the Sierra Nevada elongated dome (Betics, SE Spain): Tectonics, v. 21, 1012, doi: 10.1029/2001TC001283.

Martínez-Martínez, J.M., Soto, J.I., and Balanyá, J.C., 2004, Elongated domes in extended orogens: A mode of mountain uplift in the Betics (southeast Spain), *in* Whitney, D.L., Teyssier, C., and Siddoway, C.S., eds., Gneiss Domes in Orogeny: Geological Society of America Special Paper 380, p. 243–266.

Mather, A.E., and Harvey, A.M., 1995, Controls on drainage evolution in the Sorbas basin, southeast Spain, *in* Lewin, J., Macklin, M.G., and Woodward, J.C., eds., Mediterranean Quaternary River Environments: Rotterdam, Balkema, p. 65–76.

Morales, J., Serrano, I., Jabaloy, A., Galindo-Zaldívar, J., Zhao, D., Torcal, F., Vidal, F., and González-Lodeiro, F., 1999, Active continental subduction beneath the Betic Cordillera and the Alborán Sea: Geology, v. 27, p. 735–738, doi: 10.1130/0091-7613(1999)027<0735:ACSBTB>2.3.CO;2.

Muñoz, D., Cisternas, A., Udías, A., Mezcua, J., Sanz de Galdeano, C., Morales, J., Sánchez-Venero, M., Haessler, H., Ibañez, J., Buforn, E., Pascual,

G., and Rivera, L., 2002, Microseismicity and tectonics in the Granada Basin (Spain): Tectonophysics, v. 356, p. 233–252, doi: 10.1016/S0040-1951(02)00338-4.

Nash, D.J., and McLaren, S.J., 2003, Kalahari valley calcretes: Their nature, origins, and environmental significance: Quaternary International, v. 111, p. 3–22, doi: 10.1016/S1040-6182(03)00011-9.

Nash, D.J., and Smith, R.F., 2003, Properties and development of channel calcretes in a mountain catchment, Tabernas Basin, southeast Spain: Geomorphology, v. 50, p. 227–250, doi: 10.1016/S0169-555X(02)00216-7.

Ortiz, J.E., Torres, T., Julià, R., Delgado, A., Lamas, F.J., Soler, V., and Delgado, J., 2004, Numerical dating algorithms of amino acid racemization ratios from continental ostracodes: Application to the Guadix-Baza basin (southern Spain): Quaternary Science Reviews, v. 23, p. 717–730, doi: 10.1016/j.quascirev.2003.06.001.

Peña, J., 1979, La depresión de Guadix-Baza: Estratigrafía del Plioceno-Pleistoceno [Ph.D. thesis]: Granada, Universidad de Granada, 160 p.

Pérez-Folgado, M., Sierro, F.J., Flores, J.A., Cacho, I., Grimalt, J.O., Zahn, R., and Shackleton, N.J., 2003, Western Mediterranean planktonic foraminifera events and millennial variability during the last 70 kyr: Marine Micropaleontology, v. 48, p. 49–70, doi: 10.1016/S0377-8398(02)00160-3.

Quade, J., Cerling, T.E., and Bowman, J.R., 1989, Systematic variations in the carbon and oxygen isotopic composition of pedogenic carbonates along elevation transects in the southern Great Basin, United States: Geological Society of America Bulletin, v. 101, p. 464–475, doi: 10.1130/0016-7606(1989)101<0464:SVITCA>2.3.CO;2.

Sánchez Goñi, M.F., Cacho, I., Turon, J.L., Guiot, J., Sierro, F.J., Peypouquet, J.P., Grimalt, J.O., and Shackleton, N.J., 2002, Synchroneity between marine and terrestrial responses to millennial scale climatic variability during the last glacial period in the Mediterranean region: Climate Dynamics, v. 19, p. 95–105, doi: 10.1007/s00382-001-0212-x.

Sancho, C., and Meléndez, A., 1992, Génesis y significado ambiental de los caliches Pleistocenos de la región del Cinca (Depresión del Ebro): Revista de la Sociedad Geológica de España, v. 5, p. 81–93.

Sancho, C., Peña, J.L., Lewis, C., McDonald, E., and Rodes, E., 2004, Registros fluviales y glaciares Cuaternarios en las cuencas de los Ríos Cinca y Gállego (Pirineos y depresión del Ebro): Geo-Guías, v. 1, p. 181–205.

Sanyal, P., Bhattacharya, S.K., Kumar, R., Ghosh, S.K., and Sangode, S.J., 2004, Mio-Pliocene monsoonal record from Himalayan foreland basin (Indian Siwalik) and its relation to vegetational change: Palaeogeography, Palaeoclimatology, Palaeoecology, v. 205, p. 23–41, doi: 10.1016/j.palaeo.2003.11.013.

Sanz de Galdeano, C., and Alfaro, P., 2004, Tectonic significance of the present relief of the Betic Cordillera: Geomorphology, v. 63, p. 175–190, doi: 10.1016/j.geomorph.2004.04.002.

Sanz de Galdeano, C., Peláez-Montilla, J.A., and López-Casado, C., 2003, Seismic potential of the main active faults in the Granada Basin (southern Spain): Pure and Applied Geophysics, v. 160, p. 1537–1556, doi: 10.1007/s00024-003-2359-3.

Serrano, I., Zhao, D., and Morales, J., 2002, 3-D crustal structure of the extensional Granada basin in the convergent boundary between the Eurasian and African plates: Tectonophysics, v. 344, p. 61–79, doi: 10.1016/S0040-1951(01)00201-3.

Silva, P.G., Goy, J.L., Zazo, C., and Bardají, T., 2003, Fault-generated mountain fronts in southeast Spain: Geomorphologic assessment of tectonic and seismic activity: Geomorphology, v. 50, p. 203–225, doi: 10.1016/S0169-555X(02)00215-5.

Vandekerckhove, L., Poesen, J., Oostwoud Wijdenes, D., Gyssels, G., Beuselinck, L., and de Luna, E., 2000, Characteristics and controlling factors of bank gullies in two semi-arid Mediterranean environments: Geomorphology, v. 33, p. 37–58, doi: 10.1016/S0169-555X(99)00109-9.

Vandekerckhove, L., Poesen, J., and Govers, G., 2003, Medium-term gully headcut retreat rates in southeast Spain determined from aerial photographs and ground measurements: CATENA, v. 50, p. 329–352, doi: 10.1016/S0341-8162(02)00132-7.

Vera, J.A., 1970, Estudio estratigráfico de la depresión de Guadix-Baza: Boletín Geológico y Minero, v. 81, p. 429–462.

Verrecchia, E.P., Freytet, P., Verrecchia, K.E., and Dumont, J.L., 1995, Spherulites in calcrete laminar crusts: Biogenic $CaCO_3$ precipitation as a major contributor to crust formation: Journal of Sedimentary Research, v. 65, p. 690–700.

Viseras, C., 1991, Estratigrafía y sedimentología del relleno aluvial de la Cuenca de Guadix (Cordilleras Béticas) [Ph.D. thesis]: Granada, Universidad de Granada, 327 p.

Viseras, C., and Fernández, J., 1992, Sedimentary basin destruction inferred from the evolution of drainage systems in the Betic Cordillera, southern Spain: Journal of the Geological Society of London, v. 149, p. 1021–1029.

Watts, N.L., 1980, Quaternary pedogenic calcretes from the Kalahari (southern Africa): Mineralogy, genesis and diagenesis: Sedimentology, v. 27, p. 661–686.

Zanchetta, G., Di Vito, M., Fallick, A.E., and Sulpizio, R., 2000, Stable isotopes of pedogenic carbonates from the Somma-Vesuvius area, southern Italy, over the past 18 kyr: Palaeoclimatic implications: Journal of Quaternary Science, v. 15, p. 813–824, doi: 10.1002/1099-1417(200012)15:8<813::AID-JQS566>3.0.CO;2-Z.

Manuscript Accepted by the Society 17 May 2006

Geological Society of America Special Papers

Calcrete features and age estimates from U/Th dating: Implications for the analysis of Quaternary erosion rates in the northern limb of the Sierra Nevada range (Betic Cordillera, southeast Spain)

J.M. Azañón, P. Tuccimei, A. Azor, et al.

Geological Society of America Special Papers 2006;416; 223-239
doi:10.1130/2006.2416(14)

Notes